Construction of ceRNA networks with different types of *IDH1* mutation status in low-grade glioma patients

Wen-Jie Wang[1#], Yu-Jie Lu[2#], Ying Li[1#], Jie-Qing Tang[2], Han Wang[3], Wei Song[4], Jing-Jing Wang[5], Yue-Qing Huang[6], Ying Wang[2], Lian Lian[7]

[1]Department of Radio-Oncology, Suzhou Municipal Hospital, The Affiliated Suzhou Hospital of Nanjing Medical University, Suzhou, China; [2]Department of Oncology, Suzhou Municipal Hospital, The Affiliated Suzhou Hospital of Nanjing Medical University, Suzhou, China; [3]Department of Oncology, Jining Cancer Hospital, Jining, China; [4]Department of Gastrointestinal Surgery II, Renmin Hospital of Wuhan University, Wuhan, China; [5]Department of Intensive Care Unit, Changzhou Traditional Chinese Medical Hospital, Changzhou, China; [6]Department of General Medicine, Suzhou Municipal Hospital, The Affiliated Suzhou Hospital of Nanjing Medical University, Suzhou, China; [7]Department of Oncology, Suzhou Xiangcheng People's Hospital, Suzhou, China

Contributions: (I) Conception and design: WJ Wang, Y Wang, L Lian; (II) Administrative support: Y Wang, L Lian; (III) Provision of study materials or patients: WJ Wang, YJ Lu, Y Li; (IV) Collection and assembly of data: JQ Tang, H Wang, W Song, JJ Wang; (V) Data analysis and interpretation: WJ Wang, YJ Lu, Y Li; (VI) Manuscript writing: All authors; (VII) Final approval of manuscript: All authors.

[#]These authors contributed equally to this work.

Correspondence to: Ying Wang. Department of Oncology, Suzhou Municipal Hospital, 26 Daoqian Street, Suzhou 215001, China. Email: wangyingmaodoululu@163.com; Lian Lian. Department of Oncology, Suzhou Xiangcheng People's Hospital, Suzhou 215001, China. Email: dr_lianlian@163.com.

Background: Isocitrate dehydrogenase 1 (*IDH1*) mutation status is related to the prognosis and immune microenvironment of glioma. Long non-coding ribonucleic acids (lncRNAs) interact with microRNAs (miRNAs), and play roles in the competitive endogenous RNA (ceRNA) network and tumor progression.

Methods: Data on low-grade glioma (LGG) *IDH1* mutation was acquired from The Cancer Genome Atlas (TCGA). An empirical analysis of differential gene expression was conducted to identify differentially expressed mRNAs (DEmRNAs), differentially expressed miRNAs (DEmiRNAs), and differentially expressed lncRNAs (DElncRNAs). Survival-associated genes were identified by a univariate Cox regression analysis. An enrichment analysis was conducted to explore the gene ontology and pathways of the DEmRNAs.

Results: Eighty-eight DEIDH1mRNAs, 88 DEIDH1lncRNAs, and 6 DEIDH1miRNAs were identified to construct a ceRNA network of LGG patients. Validated by Chinese Glioma Genome Atlas and our LGG patients of gene expression and survival, and the colorectal neoplasia differentially expressed (*CRNDE*), HOXA transcript antisense RNA, myeloid-specific 1 (*HOTAIRM1*)/miRNA-206a/hepatocyte nuclear factor 4 (*HNF4G*) axis was determined.

Conclusions: We established a ceRNA network by integrating the different *IDH1* mutation statuses of LGG patients, and identified *HNF4G*, *CRNDE*, and *HOTAIRM1* as genes related to the prognosis of and immune infiltration in LGG patients. Our findings suggest that these genes may be targets for LGG treatment, especially for patients with the wild-type *IDH1* gene variants.

Keywords: Low-grade glioma (LGG); competitive endogenous RNA (ceRNA); IDH1 mutation

Submitted Dec 06, 2021. Accepted for publication Feb 11, 2022.
doi: 10.21037/atm-21-6983
View this article at: https://dx.doi.org/10.21037/atm-21-6983

Introduction

Glioma is the most common brain carcinoma, and is divided into low-grade glioma (LGG) and high-grade glioma (HGG) (1). Under the classification system of the World Health Organization (WHO), LGG includes grade II and III gliomas (2). The 5-year survival rate of LGG is significantly higher than that of HGG, which can reach 80% (3).

In recent years, molecular diagnosis has become an integral part of LGG diagnosis. About 75% of LGG patients carry isocitrate dehydrogenase 1 (*IDH1*) mutation and that *IDH1* mutation status is associated with the prognosis of LGG patients (4,5), so a complete diagnosis and prognostic assessment of gliomas should include *IDH1* mutation status (6,7). *IDH1* is a key enzyme in the glucose metabolism pathway, which can catalyze the oxidative decarboxylation of isocitrate to α-ketoglutarate, and protect cells from oxidative stress (4). It was proved that high glucose metabolism status promotes glioma cell growth by upregulating the expression and function of growth factor receptors (8). Berghoff *et al.* (9) found that *IDH1* mutation status in LGG is closely related to the tumor immune microenvironment. Patients with mutated *IDH1* have higher immune cell infiltration and higher programmed cell death-ligand 1 (PD-L1) expression levels than patients with non-mutated *IDH1* (9). A previous study has found evidence of an association between *IDH1* mutation status and cluster of differentiation (CD)8$^+$ T cells or immune responses (10).

Salmena *et al.* (11) proposed the competitive endogenous RNA (ceRNA) hypothesis, which holds that different ribonucleic acids (RNAs), such as messenger RNA (mRNA), long non-coding RNA (lncRNA), and other pseudogenes competitively combine with the corresponding micro RNA (miRNA) to form a large-scale regulatory network. This endogenous competitive relationship can affect the biological behavior of tumors. LncRNAs are RNAs >200 bp in length that do not encode proteins (12,13). LncRNAs serve as ceRNAs, share a common functionality in regulating gene expression and encoding miRNAs, and have important roles in oncogenesis and tumor progression (12,13).

In this paper, we aimed to construct a ceRNA network to identify differentially expressed genes (DEGs) between patients' samples containing mutated *IDH1* and wild-type *IDH1* gene variants. We believe that our study makes a significant contribution to the literature because we conducted the first ever large-scale analysis of differential gene expression in glioma patients with differential genetic background establishing ceRNA regulatory networks. We hope that this information will be helpful in identifying immune cell infiltration-associated mRNAs and lncRNAs as potential treatment targets for patients with LGG containing wild-type *IDH1* gene variants.

We present the following article in accordance with the STREGA reporting checklist (available at https://atm.amegroups.com/article/view/10.21037/atm-21-6983/rc).

Methods

Patient data

A total of 30 pairs of LGG tissue samples and adjacent normal tissue samples were obtained from patients at the Affiliated Suzhou Hospital of Nanjing Medical University; none of the patients had undergone radiotherapy or chemotherapy before surgery. All procedures performed in this study were in accordance with the Declaration of Helsinki (as revised in 2013). The study was approved by ethics board of the Affiliated Suzhou Hospital of Nanjing Medical University (No. KL901199) and informed consent was taken from all the patients.

Data collection and analysis

RNA sequencing (RNA-Seq) data and the corresponding clinical information of the LGG patients was obtained from The Cancer Genome Atlas (TCGA) database (https://portal.gdc.cancer.gov/repository) and Chinese Glioma Genome Atlas (CGGA) data portal (http://www.cgga.org.cn/download.jsp). The mRNA, lncRNA, and miRNA sequence information was obtained from the Illumina HiSeqmiRNASeq and Illumina HiSeqRNASeq platforms. Five hundred and thirty LGG tissue samples and 5 normal samples were obtained from TCGA, and 139 LGG tissue samples and 4 normal samples were obtained from CGGA. We obtained a list of immune-related genes from the Immunology Database and Analysis Portal system (ImmPort, https://www.immport.org).

Identification of DERNA

The method used to identify DEGs was the same as that described in our previous article (14). The DEGs were allocated to the following two groups: (I) the different *IDH1* mutation status group (lncRNA (DE^{IDH1}lncRNA), mRNA (DE^{IDH1}mRNA), and miRNA (DE^{IDH1}miRNA)); and (II) the LGG normal group (lncRNA (DE^{LGG}lncRNA), and mRNA

(DE^{LGG}mRNA)). The cutoff criteria were as follows; $|\log_2$ fold Change$|$ >1.0, and a P value <0.05.

Establishment of the ceRNA network

The relationship between lncRNA and miRNA was identified by the miRcode database, and the sequence information of the miRNAs was obtained from the StarBase v2.0 database. The TargetScan and miRDB databases provided the investigators with information about the miRNA and mRNA interactions (15,16). mRNAs that could be searched in both databases were defined as the candidate mRNAs. Next, the candidate mRNAs were intersected with the differentially expressed mRNAs to identify the mRNAs targeted by the DEmiRNAs. Next, a ceRNA network of DEGs based on the DEmiRNA-DElncRNA and DEmiRNA-DEmRNA interactions was established using Cytoscape 3.7.2 (17,18).

Functional enrichment analysis

The Gene Ontology (GO) and Kyoto Encyclopedia of Genes and Genomes analyses were conducted using R package to clarify the functional enrichment of genes in the ceRNA network. The cutoff P value for the GO and KEGG analyses was <0.05.

Survival analysis

We identified the prognostic mRNA, LncRNA, and miRNA based on a univariate Cox analysis. For a further analysis of the survival prognosis, we constructed Kaplan-Meier plots, and used the log-rank test for the statistical analysis.

The immune cell infiltration status of TCGA LGG patients

We downloaded the immune cell infiltration data of LGG patients from the TIMER website (https://cistrome.shinyapps.io/). TIMER is an open website that contains over 10,000 samples of about 30 cancer types with 6 types of immune cell infiltration from TCGA, including $CD8^+$ T cells, B cells, $CD4^+$ T cells, neutrophils, macrophages, and dendritic cells (DCs) (19).

Quantitative real-time PCR

Total RNA was isolated from the samples of 30 LGG patients by TRIzol reagent (Invitrogen, USA), and reverse transcribed using a First Strand cDNA Synthesis Kit (New England Biolabs, China). RNA amplification was performed using a SYBR Green polymerase chain reaction (PCR) kit (Applied Biological Materials, Canada) based on the Applied Biosystems 7500Real-Time PCR System (Applied Biosystems, USA). The $2^{-\Delta\Delta Ct}$ method was used to normalize the expression of RNA. The PCR primers in this study are shown in Table S1; three independent experiments were conducted.

Statistical analyses

All the statistical analyses were performed using SPSS 23.0 (Chicago, USA) and GraphPad Prism 8.0 (San Diego, USA) software. A Spearman's rank analysis was conducted to examine the association between gene expression and immune cell infiltration. The Student's *t*-test was used to analyze differences between the groups, and a univariate Cox regression analysis was conducted to identify the prognostic genes. A P value <0.05 was considered statistically significant.

Results

Clinical features of LGG patients

A total of 30 LGG patients were included in our study, of whom 15 had *IDH1* mutations and 15 had wild-type *IDH1*gene variants. The clinical features of TCGA and CGGA patients are shown in *Table 1*. Of the 530 TCGA patients, patients with no overall survival (OS) data and those with *IDH1* mutation status were removed, and subsequently, our research database comprised 506 patients (225 female and 281 male, with a median age of 41 (range, 14–87 years). Two hundred and forty-three patients had grade II LGG, and 263 had grade III LGG. Three hundred and eighty-nine patients had the *IDH1* mutation, and 117 patients had the wild-type *IDH1* form. The wild-type *IDH1* patients had worse OS than the *IDH1* mutation patients (see Figure S1A).

The CGGA validation data set comprised 182 patients with primary LGG. Among them, 71 were female and 111 were male. The patients had a median age of 39 (range, 10–74) years. One hundred and three patients had grade II LGG and 79 had grade III LGG. 133 patients had a mutation in the *IDH1* gene, 48 had a normal form of *IDH1*, and 1 had unknown mutational status. The wild-

Table 1 The clinical features of LGG patients in TCGA and CGGA

Clinical features	TCGA (N=506)	CGGA (N=182)
Age (years)		
Median	41	39
Range	14–87	10–74
Gender, n (%)		
Female	225 (44.47)	71 (39.01)
Male	281 (55.53)	111 (60.99)
Grade, n (%)		
G2	243 (48.02)	103 (56.59)
G3	263 (51.98)	79 (43.41)
IDH1 mutation, n (%)		
Mutant	389 (76.88)	133 (73.08)
Wild-type	117 (23.22)	48 (26.37)
Unknown	0	1 (0.55)

LGG, low-grade glioma; CGGA, Chinese Glioma Genome Atlas; IDH1, isocitrate dehydrogenase 1; LGG, low-grade glioma; TCGA, The Cancer Genome Atlas.

type *IDH1* patients had worse OS than the *IDH1* mutation patients (see Figure S1B).

Identified DE^{IDH1}lncRNAs, DE^{IDH1}miRNAs, and DE^{IDH1}mRNAs in LGG patients with different IDH1 mutation statuses

The DEGs^{IDH1} for 113 LGG tissue samples with wild-type *IDH1* and the DEGs for 398 LGG tissue samples with mutated *IDH1* were identified as significant by the "DESeq" R package. After the analysis, we identified 2,196 DE^{IDH1}mRNAs (302 upregulated and 1,894 downregulated) (*Figure 1A*), 1,294 DE^{IDH1}lncRNAs (328 upregulated and 966 downregulated) (*Figure 1B*), and 29 DE^{IDH1}miRNAs (7 upregulated and 22 downregulated) (*Figure 1C*). The distribution of all DEGs in the 2 ranges of -log (false discovery rate (FDR)) and logFC are shown in the volcano map in *Figures 1A-1C*. The heatmap is shown in *Figure 1D-1F*.

Establishment of the ceRNA network

To analyze the mechanism by which lncRNA mediates mRNA regulation by binding to miRNAs in LGG patients with different *IDH1* mutational statuses, a network containing related lncRNAs, miRNAs, and mRNAs (the ceRNA network) was established and visualized by Cytoscape. A total of 1,294 DE^{IDH1}lncRNAs were obtained from the miRcode database, and 177 pairs of interacting lncRNAs and miRNAs were identified by the Perl program. The target mRNAs of the 6 miRNAs were identified by the TargetScan and miRDB databases. The mRNAs included in the two gene sets were finally selected, and the mRNAs excluded in the DEmRNA gene set were removed. As a result, 88 DE^{IDH1}mRNAs were identified in the ceRNA network (see Figure S2). Overall, a total of 88 DElncRNAs, 6 DEmiRNAs, and 88 DEmRNAs were included in the ceRNA network (see *Figure 2*).

Functional enrichment analysis of DEmRNAs in the ceRNA network

The biological functions of 88 DE^{IDH1}mRNAs were examined via GO and KEGG analyses. A total of 38 biological process categories were identified in the GO analysis (P<0.05), and 5 significantly enriched pathways were found (see *Figure 3A* and Table S2). The most enriched GO term was the "transcription, DNA-template". Additionally, 8 significant pathways were identified in the KEGG pathway analysis (see *Figure 3B* and Table S3). The most enriched KEGG pathway was the "phosphatidylinositol 3'-kinase (PI3K)-Akt signaling pathway."

Survival-related lncRNAs in the ceRNA network

To explore the relationship between DE^{IDH1}RNAs and the prognosis of patients with gliomas, a prognostic signature was established based on the univariate Cox regression analysis. Consequently, 65 DE^{IDH1}mRNAs, 10 DE^{IDH1}lncRNAs, and 2 DE^{IDH1}miRNAs were found to be significantly related to the outcomes of LGG patients (see *Figure 4A-4C*).

Identification of the common DE^{LGG}lncRNAs and common immune-related DE^{LGG}mRNAs, and the establishment of the relevant ceRNA network

To search further for potential therapeutic targets for LGG, we identified the DE^{LGG}lncRNAs and DE^{LGG}mRNAs in the LGG tissue samples and adjacent tissue samples (see Figure S2). The heatmaps and volcano plots of DE^{LGG}mRNAs or DE^{LGG}lncRNAs in LGG and normal

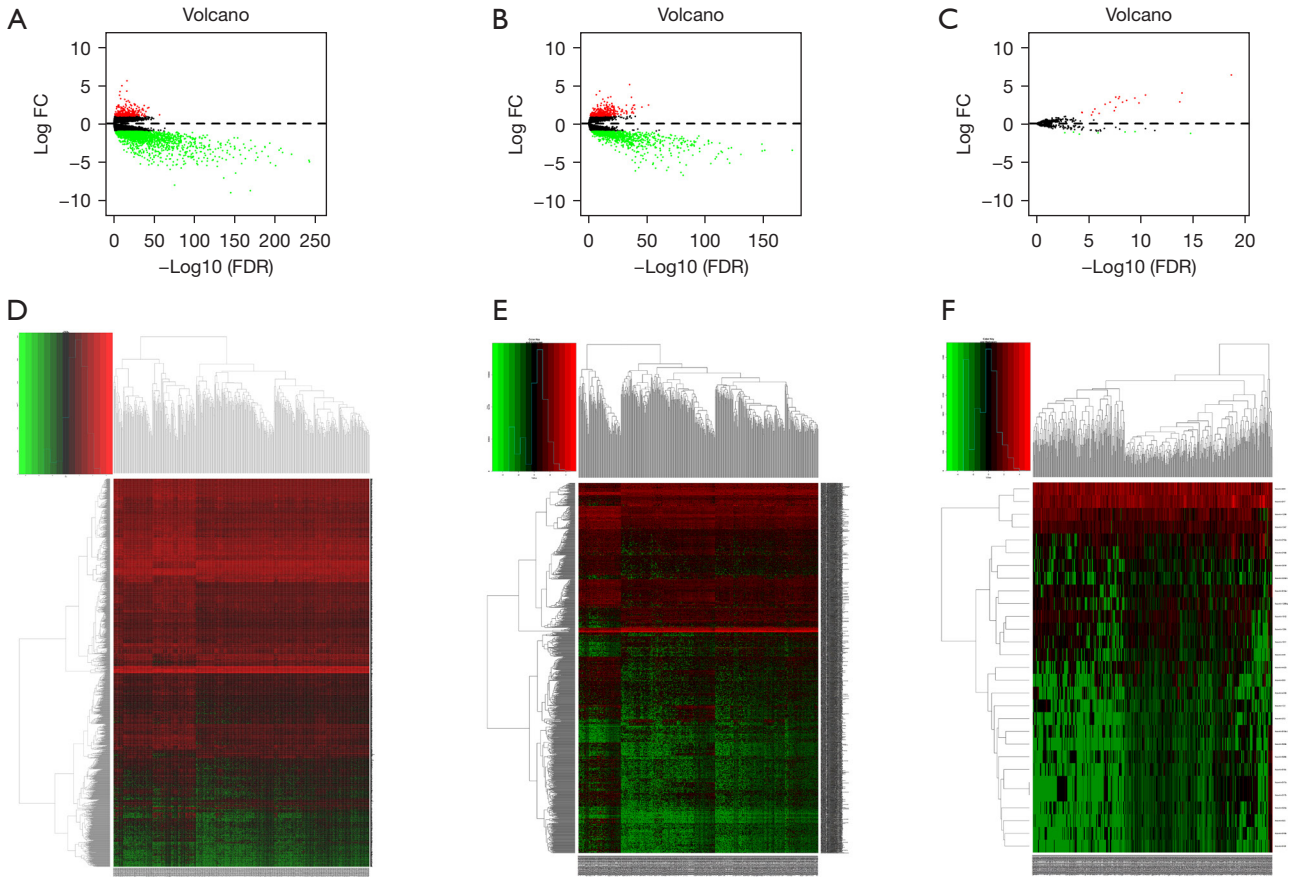

Figure 1 Identification of the DE^{IDH1}lncRNAs, DE^{IDH1}miRNAs, and DE^{IDH1}mRNAs in LGG patients with different *IDH1* mutational statuses: Volcano plot of differentially expressed mRNAs (A), lncRNAs (B) and miRNAs (C). The red point in the plot represents upregulated RNAs, and the green point represents downregulated RNAs of statistical significance. Heatmap of differentially expressed mRNAs (D), lncRNAs (E) and miRNAs (F). In *Figure 1A-1C*, the red and green dots represent upregulated and downregulated genes, respectively. LGG, low-grade glioma.

tissue samples were shown in Figure S3. Next, we interpolated the DEmRNAs, the prognostic-related DE^{IDH1}mRNAs, and the immune-related genes to obtain 2 mRNAs [i.e., Hepatocyte nuclear factor 4 (*HNF4G*) and angiopoietin like 2 (*ANGPTL2*)] (see Figure S4A). These 2 genes may be related to LGG immunity. Five lncRNAs (i.e., the colorectal neoplasia differentially expressed (*CRNDE*), HOXA transcript antisense RNA, myeloid-specific 1 (*HOTAIRM1*), GLYCTK antisense RNA 1 (*GLYCTK-AS1*), ZBTB20 antisense RNA 4 (*ZBTB20-AS4*), and long intergenic non-protein coding RNA 519 (*LINC00519*)) were identified by intersecting the DE^{LGG}lncRNAs and the prognosis-related lncRNAs (see Figure S4B). Finally, we compared the obtained mRNAs and lncRNAs with the ceRNA network (see *Figure 2*). We found that the mRNA *HNF4G* and *ANGPTL2* and the lncRNA *CRNDE*, *HOTAIRM1*, and *GLYCTK-AS1* may interact via *miRNA204*, *miRNA216ai*, and *miRNA216b*, and thus constructed a new network (see *Figure 5*).

Validation of gene expression and prognosis in the ceRNA network

The expression and survival analysis of related genes were verified in the CGGA database. First, we verified gene expression in the CGGA database (see *Figure 6A-6E*). The expression levels of *HNF4G*, *CRNDE*, and *HOTAIRM1* in patients with mutated *IDH1* were lower than those of patients with wild-type *IDH1*, while the expression levels of *ANGPTL2* and *GLYCTK-AS1* in patients with

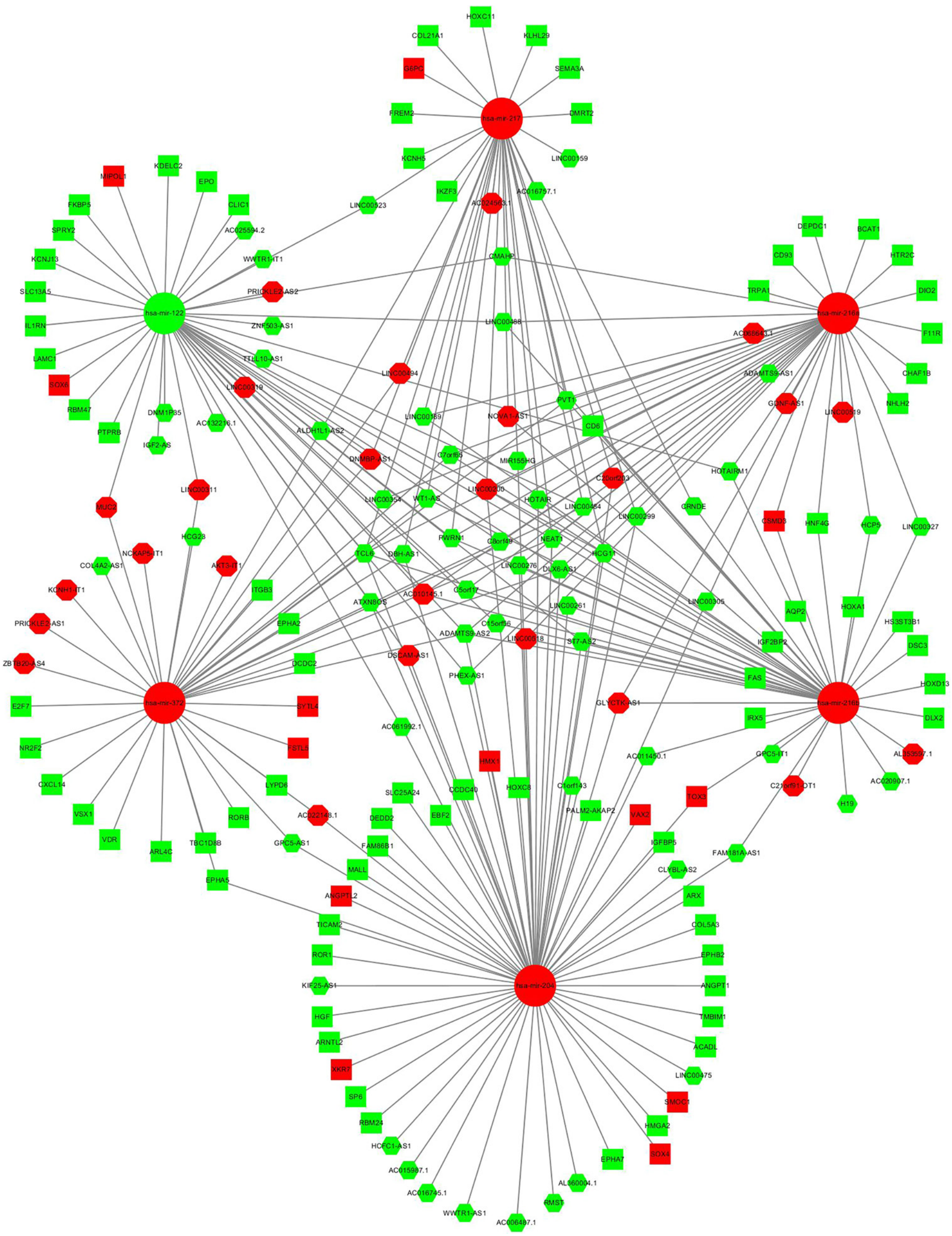

Figure 2 The ceRNA network in in LGG patients with different *IDH1* mutational statuses; the circles indicate miRNAs, the diamonds indicate lncRNA, and the octangles indicate mRNA. The red and green nodes represent upregulated and downregulated RNAs, respectively. LGG, low-grade glioma.

mutated *IDH1* were higher than those of patients with wild-type *IDH1*.

Second, we verified survival in the CGGA database. We divided the patients into two groups based on median gene expression. The higher expression group of *HNF4G* (see *Figure 7A*), *HOTAIRM1* (see *Figure 7B*), and *CRNDE* (see *Figure 7C*) had worse OS than the lower expression group. The lower expression group of *ANGPTL2* (see *Figure 7D*) had worse OS than the higher expression group. The survival analysis of these 4 genes was consistent with TCGA database. However, there was no statistically significant difference in the survival analysis of *GLYCTK-AS1* (see

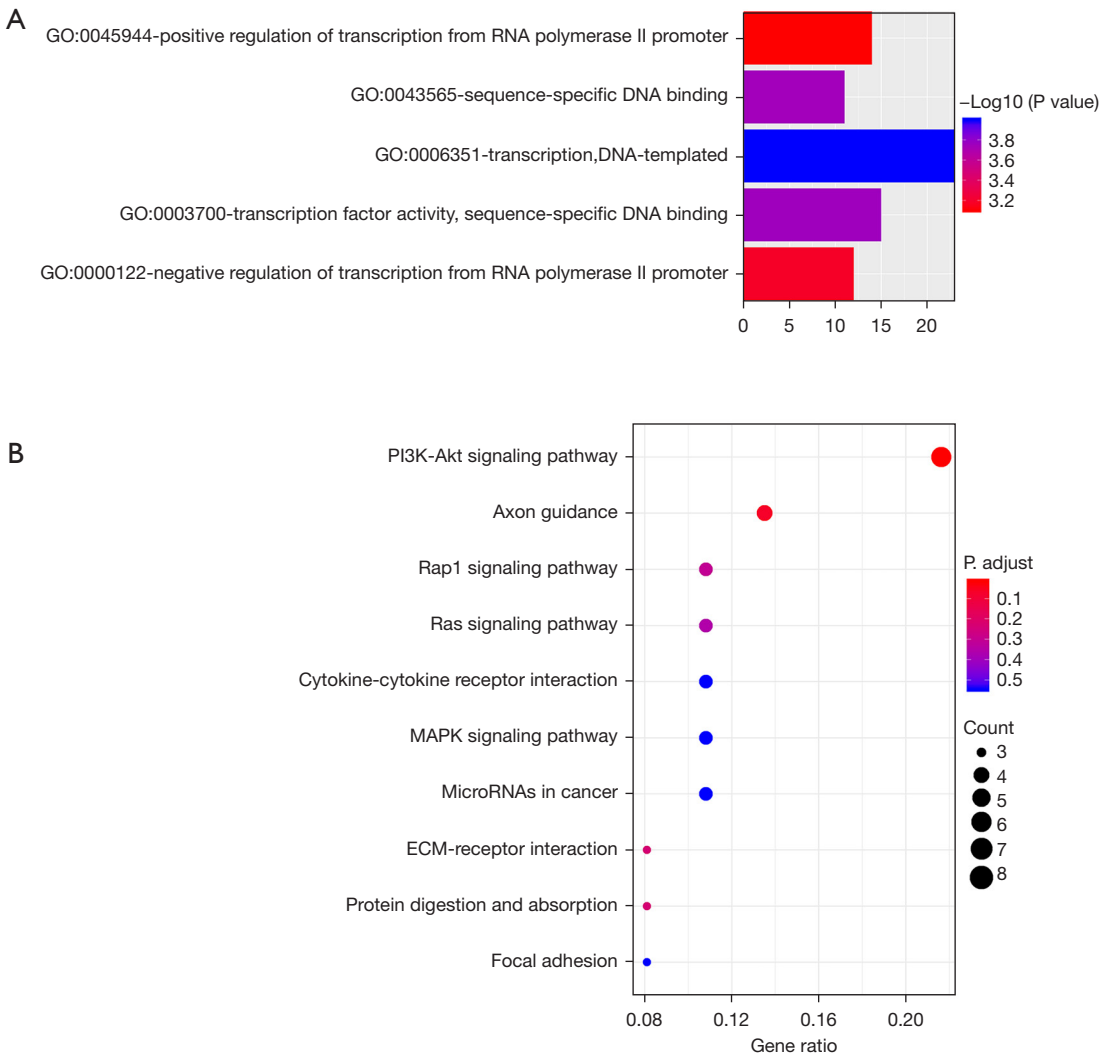

Figure 3 The enriched top 5 GO biological process terms (A) and KEGG pathway (B) of the DE^{IDH1}mRNAs involved in the ceRNA network. GO, Gene Ontology; KEGG,Kyoto Encyclopedia of Genes and Genomes.

Figure 7E). Next, we divided patients into the following four groups: (I) the low expression and *IDH1* mutant group; (II) the high expression and *IDH1* mutant group; (III) the low expression and *IDH1* wild-type group; and (IV) the high expression and *IDH1* wild-type group. The high expression and *IDH1* wild-type group of *HNF4G* (see *Figure 7F*), *HOTAIRM1* (see *Figure 7G*), *CRNDE* (see *Figure 7H*) had worse OS than the other 3 groups. The low expression and *IDH1* wild-type group of *ANGPTL2* (see *Figure 7I*) had worse OS than the other groups.

Finally, we measured expression levels using LGG patients' tissue samples and normal tissue samples. The expression levels of *HNF4G* (see *Figure 8A*), *CRNDE* (see *Figure 8B*), and *HOTAIRM1* (see *Figure 8C*) were consistent with those in TCGA and CGGA databases. The expression levels of *ANGPTL2* (see *Figure 8D*) and *GLYCTK-AS1* (see *Figure 8E*) were inconsistent with those in TCGA and CGGA databases.

Through further analysis we found that mRNA *HNF4G*, lncRNA *CRNDE*, and *HOTAIRM1* were consistent in both databases with our samples. *HNF4G* expression was positively correlated with *CRNDE* expression in both TCGA (r=0.447, P<0.001) (see Figure S5A) and CGGA (r=0.482, P<0.001; see Figure S5B) databases. *HNF4G* expression was positively related to *HOTAIRM1* expression in both TCGA (r=0.343, P<0.001; see Figure S5C) and

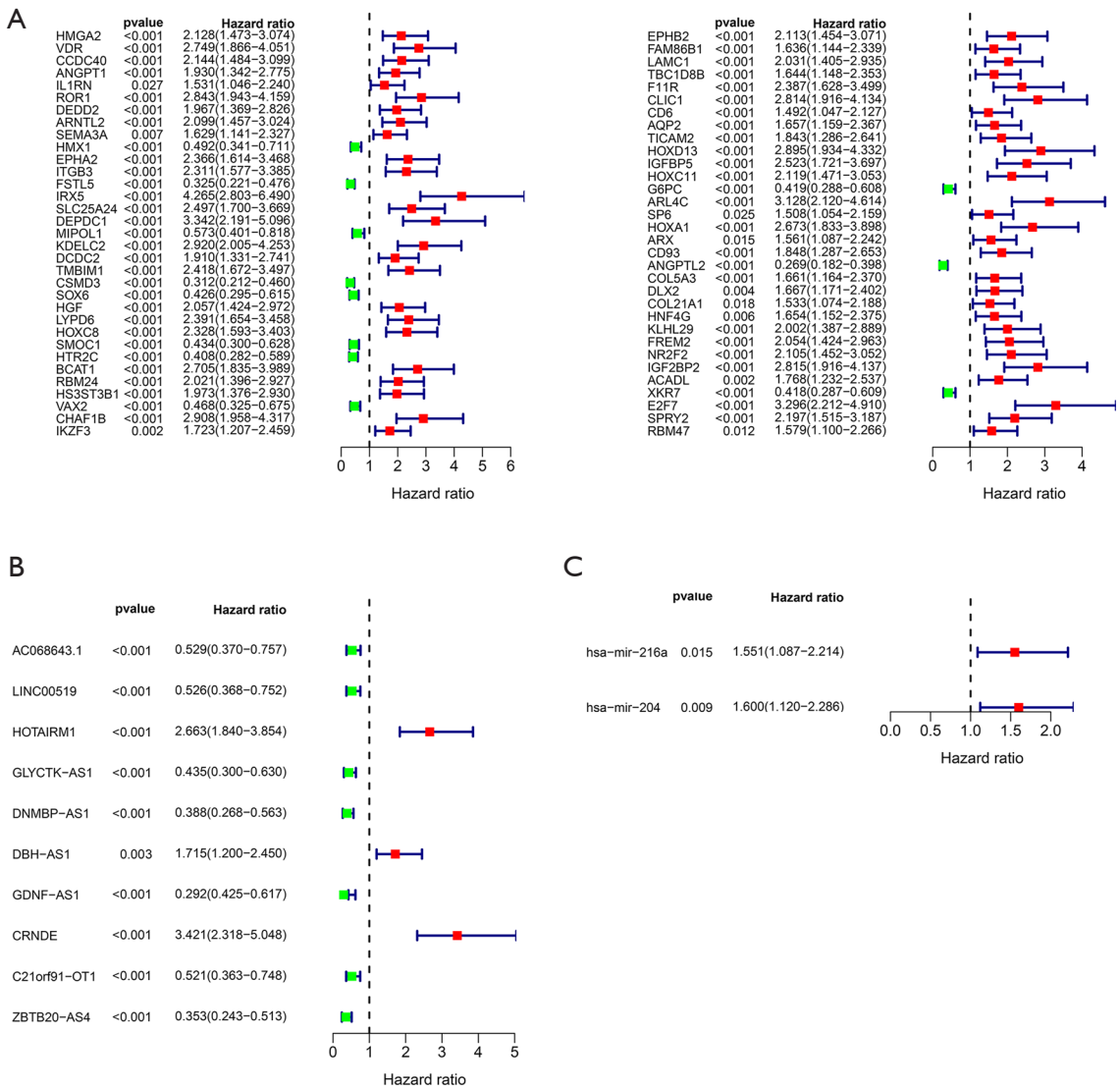

Figure 4 Prognosis-related genes: mRNAs (A), lncRNAs (B) and miRNAs (C).

CGGA (r=0.370, P<0.001; see Figure S5D) databases.

The relationship between different IDH1 mutation statuses and the expression of key genes with immune cell infiltration and PD-L1 expression

To further clarify the relationship between *IDH1* mutation status and the immune microenvironment and *PD-L1* expression, we analyzed the 6 immune cell infiltration levels in LGG patients by comparing mutated *IDH1* and wild-type *IDH1*. The LGG patients with normal *IDH1* had higher infiltration levels of 5 types of immune cells; that is, B cells (see *Figure 9A*), DCs (see *Figure 9B*), $CD8^+$ T cells (see *Figure 9C*), neutrophils (see *Figure 9D*), and macrophages (see *Figure 9E*). CD4+ T cell (see *Figure 9F*) infiltration was not significantly different between the two groups of patients. The *PD-L1* expression levels were higher in LGG patients with wild-type *IDH1* than those with mutant *IDH1* in TCGA (see *Figure 9G*) and CGGA (see *Figure 9H*) databases.

The relationship between expression of immune-related genes and DElncRNAs with immune cell infiltration are shown in *Figure 10*.

For mRNA, *HNF4G* expression was positively correlated

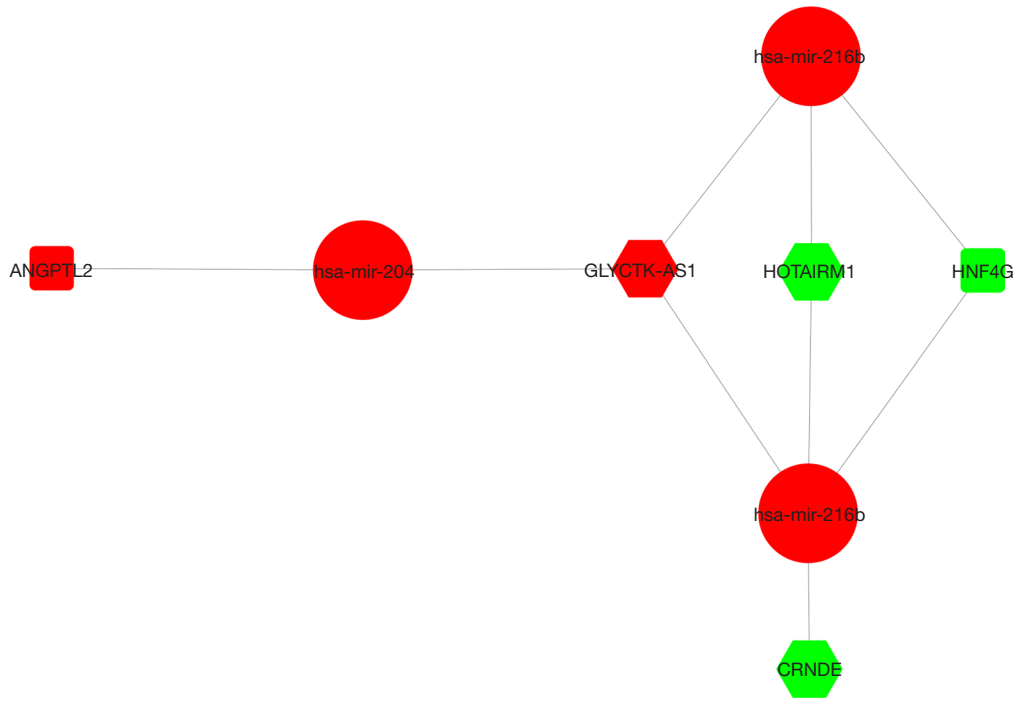

Figure 5 CeRNA network with common genes.

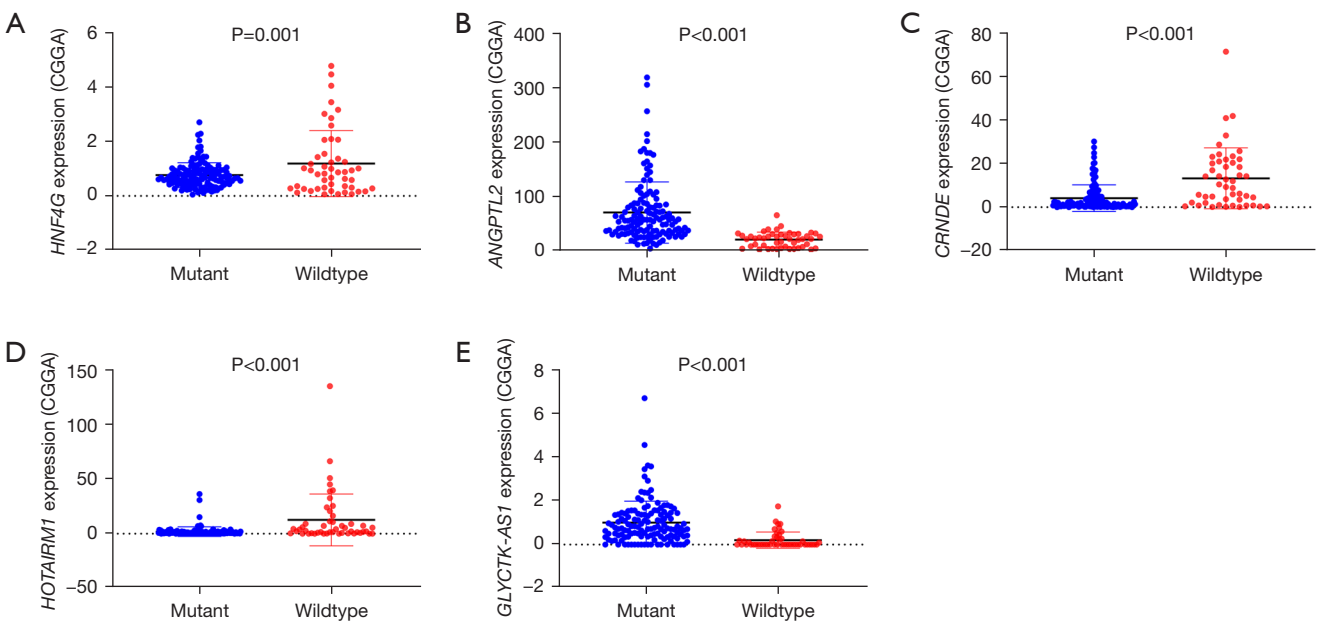

Figure 6 Verification of gene expression in the CGGA database: The expression of *HNF4G* (A), *ANGPTL2* (B), *CRNDE* (C), *HOTAIRM1* (D), *GLYCTK-AS1* (E). *CGGA*, Chinese Glioma Genome Atlas.

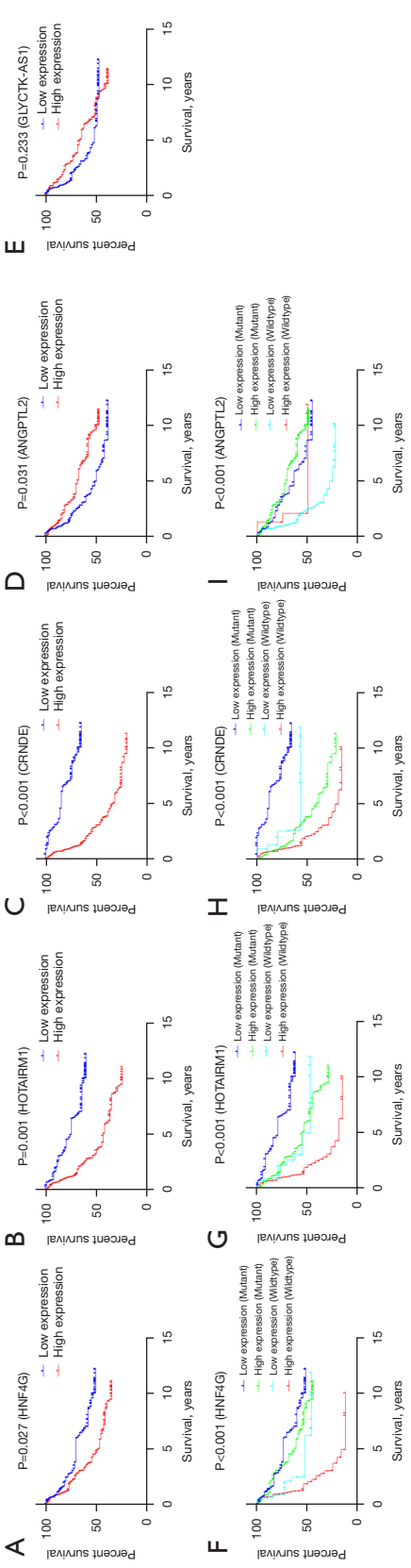

Figure 7 Verification of the survival of different gene expression groups in the CGGA database: The survival analysis of different expression groups of *HNF4G* (A), *HOTAIRM1* (B), *CRNDE* (C), *ANGPTL2* (D), *GLYCTK-AS1* (E), *HNF4G* and *IDH1* mutation status (F), *HOTAIRM1* and *IDH1* mutation status (G), *CRNDE* and *IDH1* mutation status (H), *ANGPTL2* and *IDH1* mutation status (I). CGGA, Chinese Glioma Genome Atlas.

with B cells (r=0.179, P<0.001; see *Figure 10A*), CD4$^+$ T cells (r=0.098, P=0.028; see *Figure 10B*), CD8$^+$ T cells (r=0.197, P<0.001; see *Figure 10C*), neutrophils (r=0.202, P=0.001; see *Figure 10D*), macrophages (r=0.189, P<0.001; see *Figure 10E*), and DCs (r=0.199, P<0.001; see *Figure 10F*).

For lncRNA, *HOTAIRM1* expression was positively correlated with B cells (r=0.211, P<0.001; see *Figure 10G*), CD4$^+$ T cells (r=0.101, P=0.022; see *Figure 10H*), CD8$^+$ T cells (r=0.228, P<0.001; see *Figure 10I*), neutrophils (r=0.240, P=0.001; see *Figure 10J*), macrophages (r=0.245, P<0.001; see *Figure 10K*), and DCs (r=0.226, P<0.001; see *Figure 10L*). *CRNDE* expression was positively correlated with B cells (r=0.301, P<0.001; see *Figure 10M*), CD4$^+$ T cells (r=0.161, P<0.001) (see *Figure 10N*), CD8$^+$ T cells (r=0.263, P<0.001) (see *Figure 10O*), neutrophils (r=0.281, P=0.001; see *Figure 10P*), macrophages (r=0.247, P<0.001; see *Figure 10Q*), and DCs (r=0.308, P<0.001; see *Figure 10R*).

The expression of *PD-L1* was positively related to the expression of *HNF4G* (r=0.332, P<0.001; see *Figure 11A*), *CRNDE* (r=0.240, P<0.001; see *Figure 11B*), and *HOTAIRM1* (r=0.178, P<0.001; see *Figure 11C*) in TCGA. The expression of *PD-L1* was positively related to *HNF4G* (r=0.285, P<0.001; see *Figure 11D*), however, the expression correlation between *PD-L1* with *CRNDE* (r=0.132, P=0.075; see *Figure 11E*), and *HOTAIRM1* (r=0.082, P=0.273; see *Figure 11F*) was not statistically significant in the CGGA database.

Discussion

In this article, the DEGs in LGGs with different *IDH1* mutational statuses were analyzed, and the following were identified: 2,196 DE^{IDH1}mRNAs, 1,294 DE^{IDH1}lncRNAs, and 29 DE^{IDH1}miRNAs. From these DEGs, we established a ceRNA network. Our ceRNA network comprised 88 DE^{IDH1}mRNAs, 88 DE^{IDH1}lncRNAs, and 6 DE^{IDH1}miRNAs (see *Figure 2*). Through the univariate Cox regression analysis, we identified 65 mRNAs and 10 lncRNAs that correlated with prognosis in the ceRNA network (see *Figure 4*). The functional enrichment analysis indicated that the highest enrichment of DE^{IDH1}mRNAs in the network was for the PI3K-Akt signaling pathway and transcription-DNA-template (see *Figure 3*).

Despite the rapid development of the molecular detection field in recent years, *IDH1* mutation status is still one of the most stable detection markers in gliomas (20). Kloosterhof *et al.* (4) found that *IDH1* mutation status is an important prognostic factor for gliomas. In TCGA and CGGA

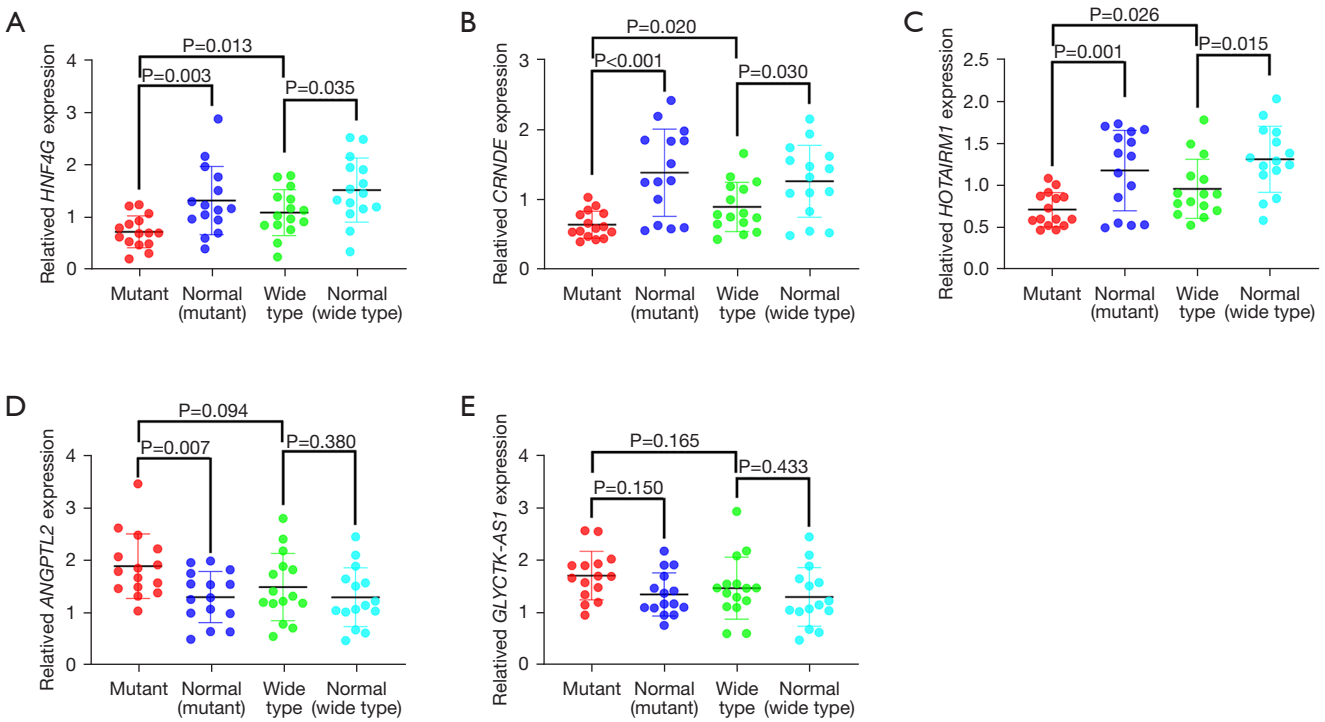

Figure 8 Verification of gene expression by using LGG tissues and adjacent normal tissues: the expression of *HNF4G* (A), *CRNDE* (B), *HOTAIRM1* (C), *ANGPTL2* (D), and *GLYCTK-AS1* (E). LGG, low-grade glioma.

databases, LGG patients with mutated *IDH1* have worse OS than those with the normal form of *IDH1*. Previously, immune cell infiltration and *PD-L1* expression were thought to be related to different types of glioma (21). However, recent research has shown that *IDH1* mutation status is also closely related to the immune microenvironment of gliomas. Berghoff *et al.* (9) showed that patients with gliomas containing wild-type *IDH1* had more prominent tumor infiltrating lymphocyte infiltration and higher PD-L1 expression than patients with mutant *IDH1*. Amankulor *et al.* found *IDH1* mutations down-regulated leukocyte chemotaxis level and then suppressed the tumor-related immune system (22). Additionally, *IDH1* mutation in glioma mediated natural killer (NK) cell resistance by epigenetic silencing of NK group 2D (*NKG2D*) (23). The analysis of LGG patients in TCGA database revealed that the infiltration of multiple immune cells in patients with wild-type *IDH1* was higher than that in those with mutated *IDH1*. Further, according to the information obtained from TCGA and CGGA databases, the expression of *PD-L1* in patients with wild-type *IDH1* was significantly higher than that of patients with mutated *IDH1*. This may indicate that different *IDH1* mutation statuses may produce different immune responses and immunotherapy effects in LGG patients.

To further analyze whether the genes in the ceRNA network are suitable for LGG and could become potential therapeutic targets for LGG, we analyzed LGG and adjacent tissues and defied DE^{LGG}mRNAs and DE^{LGG}lncRNAs. Next, we intersected these with the prognostic-related genes. A list of immune-related genes was then obtained from the ImmPort, and it was intersected with the list of identified mRNAs to identify potential immune-related genes. Finally, we identified the following 5 genes: *HNF4G* and *ANGPTL2* (mRNAs), and *CRNDE*, *HOTAIRM1*, and *GLYCTK-AS1* (lncRNAs). We then used these 5 genes to construct a new network (see *Figure 5*). Through verification with our LGG samples, we found that *HNF4G*, *CRNDE*, and *HOTAIRM1* expression levels were downregulated in patients with *IDH1* mutations (see *Figure 6*). However, their expression in glioma tissues was upregulated, which reflects the information found in TCGA and CGGA databases. Finally, we identified the *CRNDE*, *HOTAIRM1/miRNA-206a/HNF4G* axis, and found that the expression of *HNF4G* was positively correlated with *CRNDE* or *HOTAIRM1* both in TCGA and CGGA

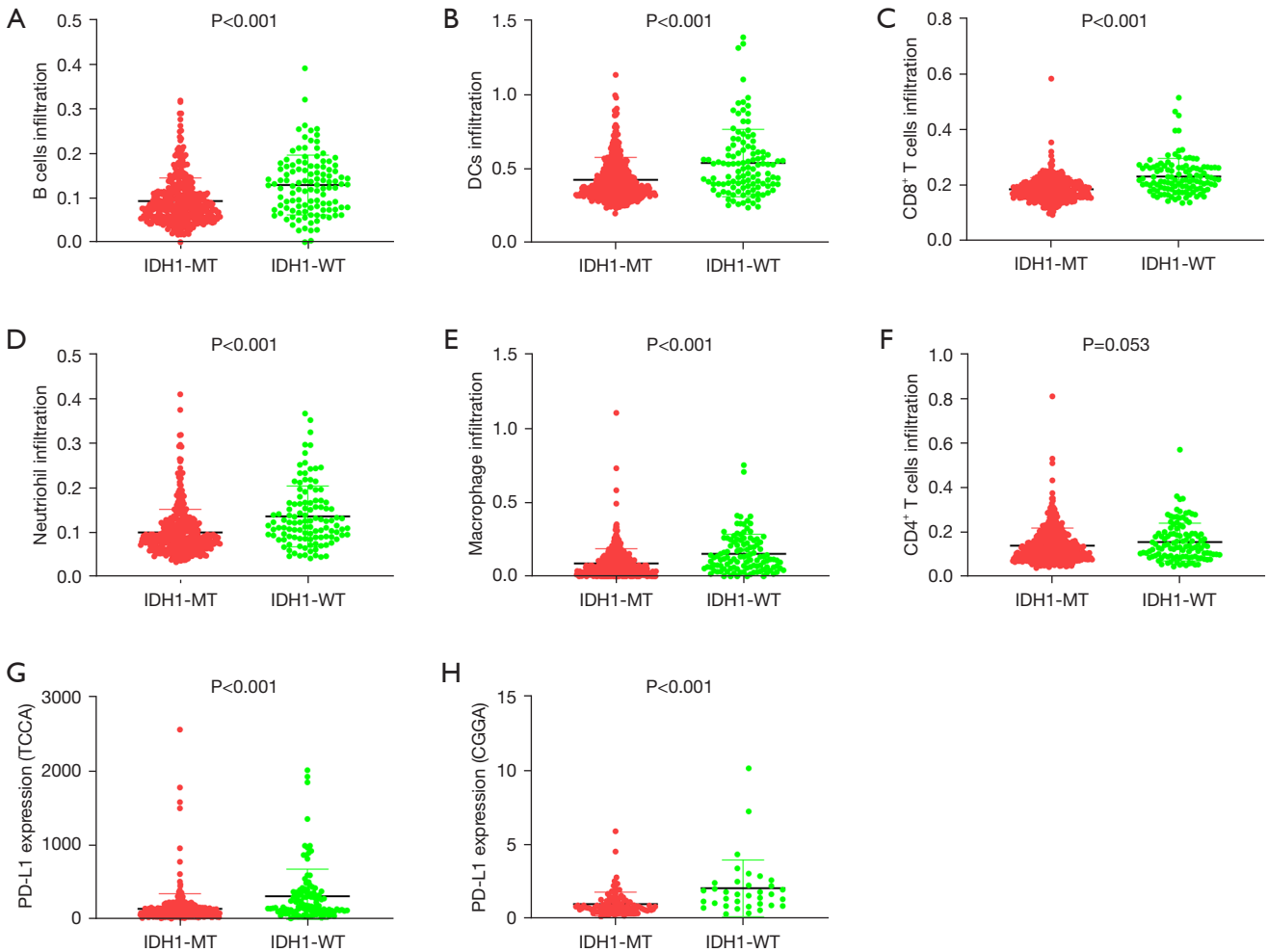

Figure 9 Relationships between different *IDH1* mutation status groups and the immune cell infiltration of B cells (A), DCs (B), $CD8^+$ T cells (C), neutrophils (D), macrophages (E), $CD4^+$ T cells neutrophils (F), PD-L1 (TCGA) (G) and PD-L1 (CGGA) (H). DCs, dendritic cells.

databases.

The relationship between the expression of these genes with immune cell infiltration and *PD-L1* expression was then analyzed. The expression levels of *HNF4G* and *CRNDE* were positively correlated to the infiltration of six types of immune cells (see *Figure 10*). The expression level of *HOTAIRM1* was positively correlated to the infiltration of 5 types of immune cells except for CD4+ T cells. The expression levels of *HNF4G*, *CRNDE*, and *HOTAIRM1* were also positively correlated to PD-L1 expression in TCGA database (see *Figure 11*). Consistent with TCGA, the expression levels of *HNF4G* were positively correlated to *PD-L1* expression in the CGGA database; however, the expression levels of *CRNDE* and *HOTAIRM1* were not statistically significantly correlated to PD-L1 expression in LGG (see *Figure 11*). Thus, *HNF4G*, *CRNDE* and *HOTAIRMI* may be closely related to immunity response.

HNF4G is a member of the orphan nuclear receptor superfamily (24). In the Chinese Han population, *HNF4G* polymorphisms are associated with ventilatory disease (25). Wang *et al.* (26) demonstrated that *HNF4G* acts as an oncogene and can promote the growth and metastasis of lung cancer cells. Further, *HNF4G* is also a prognostic factor for lung cancer. Sun *et al.* (27) found that miR-34 mediates the downregulation of *HNF4G* gene to inhibit bladder cancer cell growth and invasion. Tian *et al.* (28) demonstrated that *HOTAIRM1/HOXA1* attenuates the immunosuppressive function of myeloid-derived suppressor

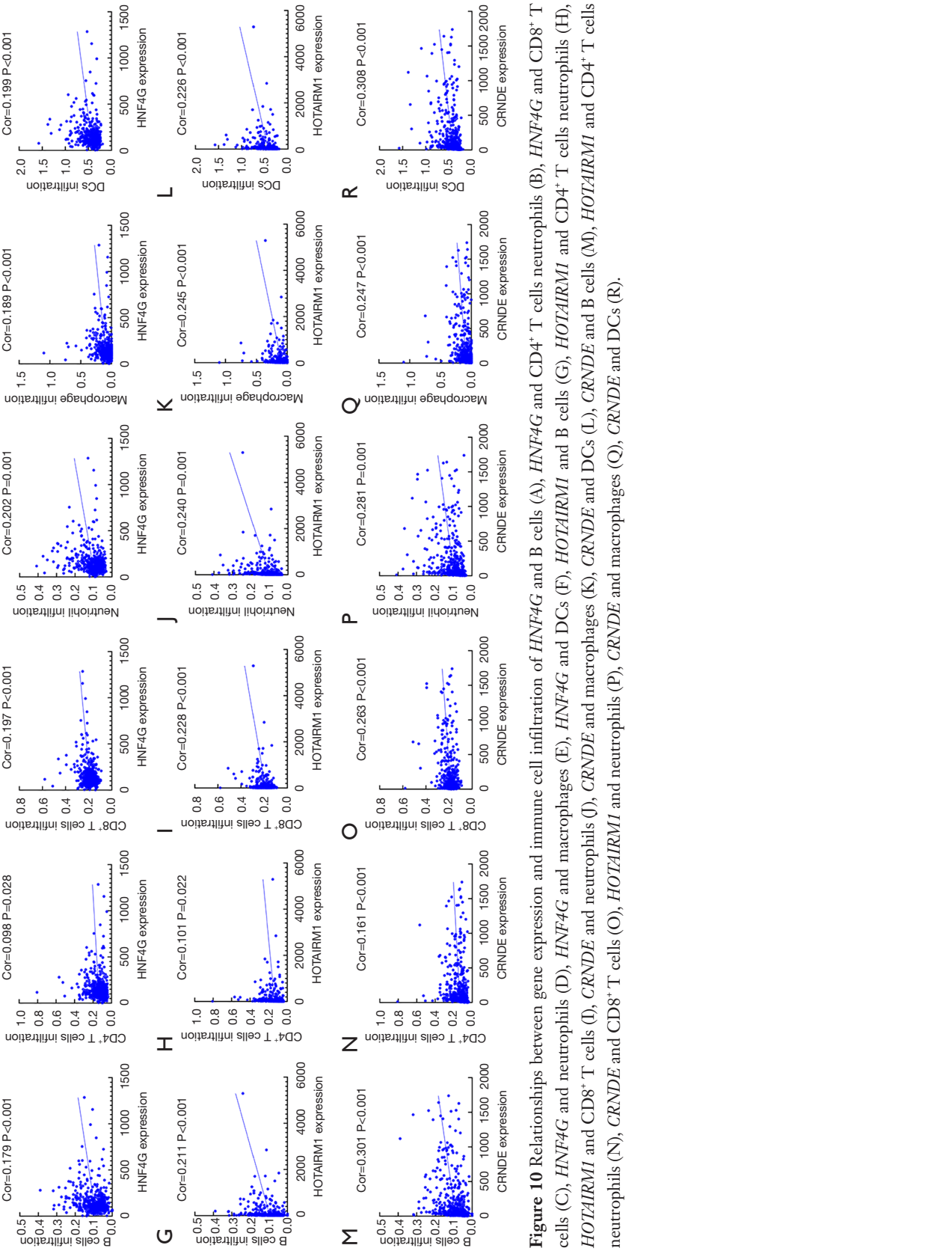

Figure 10 Relationships between gene expression and immune cell infiltration of *HNF4G* and B cells (A), *HNF4G* and $CD4^+$ T cells neutrophils (B), *HNF4G* and $CD8^+$ T cells (C), *HNF4G* and neutrophils (D), *HNF4G* and macrophages (E), *HNF4G* and DCs (F), *HOTAIRM1* and B cells (G), *HOTAIRM1* and $CD4^+$ T cells neutrophils (H), *HOTAIRM1* and $CD8^+$ T cells (I), *CRNDE* and neutrophils (J), *CRNDE* and macrophages (K), *CRNDE* and DCs (L), *CRNDE* and B cells (M), *HOTAIRM1* and $CD4^+$ T cells neutrophils (N), *CRNDE* and $CD8^+$ T cells (O), *HOTAIRM1* and neutrophils (P), *CRNDE* and macrophages (Q), *CRNDE* and DCs (R).

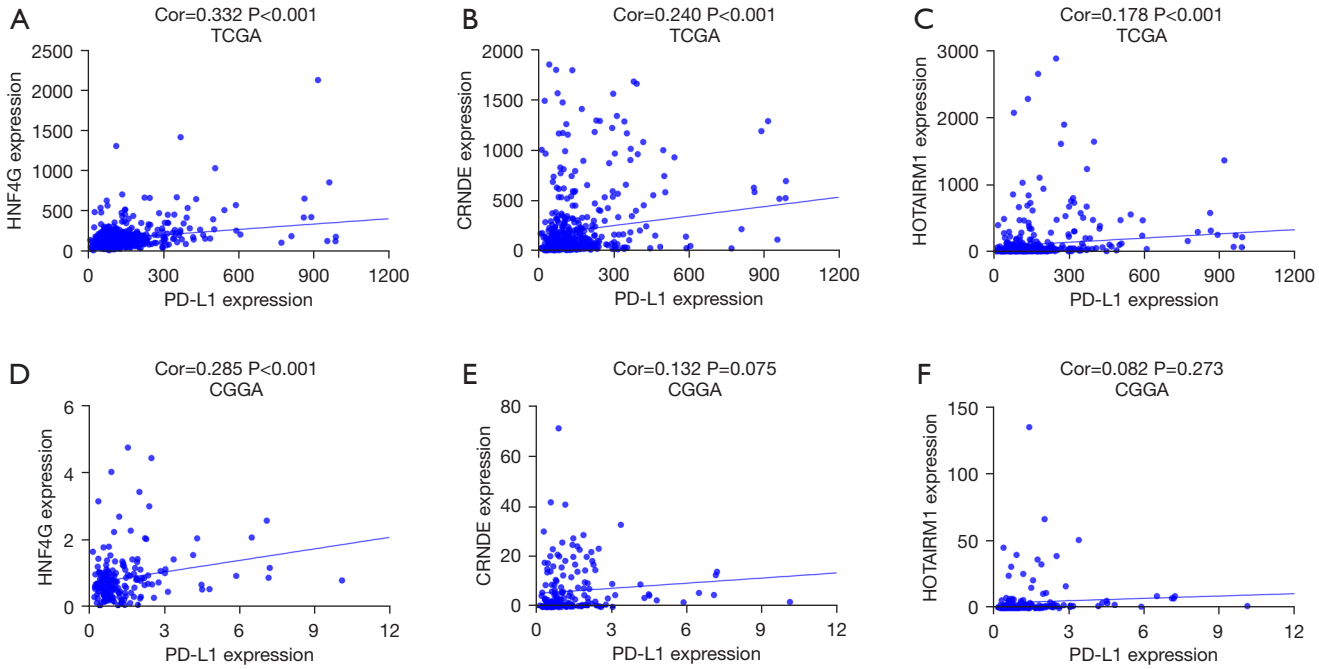

Figure 11 Relationships between expression of PD-L1 with *HNF4G*, *CRNDE* and *HOTAIRM1*: (A) expression of PD-L1 with *HNF4G* in TCGA; (B) expression of PD-L1 with *CRNDE* in TCGA; (C) expression of PD-L1 with *HOTAIRM1* in TCGA; (D) expression of PD-L1 with *HNF4G* in the CGGA; (E) expression of PD-L1 with *CRNDE* in the CGGA; (F) expression of PD-L1 with *HOTAIRM1* in the CGGA. TCGA, The Cancer Genome Atlas; CGGA, Chinese Glioma Genome Atlas.

cells in lung cancer, thereby promoting the immune response and delaying the progression of lung cancer. Lin *et al.* (29) found that *HOTAIRM1* promotes cell growth and reduces apoptosis in glioma cell lines through the miR-873-5p/ZEB2 axis. Li *et al.* (30) suggested the formation of ceRNA network by *CRNDE/MIR136-5P/Bcl-2* and Wnt2 that serves to regulate the biological characteristics of glioma. *CRNDE* can negatively regulate the miR-136-5P-mediated downregulation of Bcl-2 and Wnt2, thereby promoting the growth and metastasis of glioma cells (30). Previous studies have shown that the lncRNA *CRNDE* and *HOTAIRM1* are closely associated with the prognosis of gliomas (31,32). There are many studies on *CRNDE* and *HOTAIRM1* expression in gliomas, which indicates that these two lncRNAs are closely linked to the prognosis and biological behavior of gliomas, but there are no studies on *HNF4G* function in gliomas. The expression of *HNF4G* was positively correlated with *CRNDE* and *HOTAIRM1* in TCGA and CGGA databases, and these genes may be related to each other. In addition, the three genes are closely related to tumor growth, prognosis, and the immune microenvironment and thus may serve as targets for treating LGG patients in the near future, especially those containing wild-type *IDH1*.

Our research had some limitations. First, while we identified the *CRNDE*, *HOTAIRM1/miRNA-206a/HNF4G* axis, these genes are positively correlated with each other, and thus their interrelationships need to be further investigated. Second, the sample size was small; thus, further research needs to be conducted with a larger sample size.

In summary, through our analysis, we constructed ceRNA networks with different *IDH1* mutation statuses in LGG. By verification of the CGGA database and Quantitative Polymerase Chain Reaction (QT-PCR), we identified 1 mRNA and 2 lncRNAs that are related to immune cell infiltration and PD-L1 expression. These genes are related to LGG prognosis and *IDH1* mutational status. We believe that *HNF4G*, *CRNDE*, and *HOTAIRM1* play important roles in LGG, and these roles are related to *IDH1* mutation status and the LGG immune microenvironment. Finally, by constructing a network of these genes, any competitive relationships affecting the development of LGG may be able to be identified.

Acknowledgments

We would like to thank Wei Shan for his assistance with the statistical analyses.

Funding: This study was supported by the Science and Education for Health Foundation of Suzhou for Youth (grant No. KJXW2019074); the Science and Technology Project Foundation of Suzhou (grant Nos. SS201651, SS201852, SS202093 and SYSD2020061); Project of science and technology development plan in Suzhou (grant Nos. SYSD2018138, SYSD202006) and the Jiangsu Province Medical key discipline (grant No. ZDXKC2016007).

Footnote

Reporting Checklist: The authors have completed the STREGA reporting checklist. Available at https://atm.amegroups.com/article/view/10.21037/atm-21-6983/rc

Data Sharing Statement: Available at https://atm.amegroups.com/article/view/10.21037/atm-21-6983/dss

Conflicts of Interest: All authors have completed the ICMJE uniform disclosure form (available at https://atm.amegroups.com/article/view/10.21037/atm-21-6983/coif). All authors report funding from the Science and Education for Health Foundation of Suzhou for Youth (grant No. KJXW2019074); the Science and Technology Project Foundation of Suzhou (grant Nos. SS201651, SS201852 and SS202093); Project of science and technology development plan in Suzhou (grant Nos. SYSD2018138, SYSD202006) and the Jiangsu Province Medical key discipline (grant No. ZDXKC2016007). The authors have no other conflicts of interest to declare.

Ethical Statement: The authors are accountable for all aspects of the work in ensuring that questions related to the accuracy or integrity of any part of the work are appropriately investigated and resolved. All procedures performed in this study involving human participants were in accordance with the Declaration of Helsinki (as revised in 2013). The study was approved by ethics board of the Affiliated Suzhou Hospital of Nanjing Medical University (No. KL901199) and informed consent was taken from all the patients.

References

1. Goodenberger ML, Jenkins RB. Genetics of adult glioma. Cancer Genet 2012;205:613-21.
2. Buckner J, Giannini C, Eckel-Passow J, et al. Management of diffuse low-grade gliomas in adults - use of molecular diagnostics. Nat Rev Neurol 2017;13:340-51.
3. Wesseling P, Capper D. WHO 2016 Classification of gliomas. Neuropathol Appl Neurobiol 2018;44:139-50.
4. Kloosterhof NK, Bralten LB, Dubbink HJ, et al. Isocitrate dehydrogenase-1 mutations: a fundamentally new understanding of diffuse glioma? Lancet Oncol 2011;12:83-91.
5. SongTao Q, Lei Y, Si G, et al. IDH mutations predict longer survival and response to temozolomide in secondary glioblastoma. Cancer Sci 2012;103:269-73.
6. Cancer Genome Atlas Research Network; Brat DJ, Verhaak RG, et al. Comprehensive, Integrative Genomic Analysis of Diffuse Lower-Grade Gliomas. N Engl J Med 2015;372:2481-98.
7. Reuss DE, Kratz A, Sahm F, et al. Adult IDH wild type astrocytomas biologically and clinically resolve into other tumor entities. Acta Neuropathol 2015;130:407-17.
8. Bao Z, Chen K, Krepel S, et al. High Glucose Promotes Human Glioblastoma Cell Growth by Increasing the Expression and Function of Chemoattractant and Growth Factor Receptors. Transl Oncol 2019;12:1155-63.
9. Berghoff AS, Kiesel B, Widhalm G, et al. Correlation of immune phenotype with IDH mutation in diffuse glioma. Neuro Oncol 2017;19:1460-8.
10. Kohanbash G, Carrera DA, Shrivastav S, et al. Isocitrate dehydrogenase mutations suppress STAT1 and CD8+ T cell accumulation in gliomas. J Clin Invest 2017;127:1425-37.
11. Salmena L, Poliseno L, Tay Y, et al. A ceRNA hypothesis: the Rosetta Stone of a hidden RNA language? Cell 2011;146:353-8.
12. Peng Y, Croce CM. The role of MicroRNAs in human cancer. Signal Transduct Target Ther 2016;1:15004.
13. Tay Y, Rinn J, Pandolfi PP. The multilayered

complexity of ceRNA crosstalk and competition. Nature 2014;505:344-52.
14. Wang JJ, Huang YQ, Song W, et al. Comprehensive analysis of the lncRNA-associated competing endogenous RNA network in breast cancer. Oncol Rep 2019;42:2572-82.
15. Wong N, Wang X. miRDB: an online resource for microRNA target prediction and functional annotations. Nucleic Acids Res 2015;43:D146-52.
16. Chou CH, Chang NW, Shrestha S, et al. miRTarBase 2016: updates to the experimentally validated miRNA-target interactions database. Nucleic Acids Res 2016;44:D239-47.
17. Shannon P, Markiel A, Ozier O, et al. Cytoscape: a software environment for integrated models of biomolecular interaction networks. Genome Res 2003;13:2498-504.
18. Otasek D, Morris JH, Bouças J, et al. Cytoscape Automation: empowering workflow-based network analysis. Genome Biol 2019;20:185.
19. Bhattacharya S, Andorf S, Gomes L, et al. ImmPort: disseminating data to the public for the future of immunology. Immunol Res 2014;58:234-9.
20. Cheng W, Ren X, Zhang C, et al. Gene Expression Profiling Stratifies IDH1-Mutant Glioma with Distinct Prognoses. Mol Neurobiol 2017;54:5996-6005.
21. Garber ST, Hashimoto Y, Weathers SP, et al. Immune checkpoint blockade as a potential therapeutic target: surveying CNS malignancies. Neuro Oncol 2016;18:1357-66.
22. Amankulor NM, Kim Y, Arora S, et al. Mutant IDH1 regulates the tumor-associated immune system in gliomas. Genes Dev 2017;31:774-86.
23. Zhang X, Rao A, Sette P, et al. IDH mutant gliomas escape natural killer cell immune surveillance by downregulation of NKG2D ligand expression. Neuro Oncol 2016;18:1402-12.
24. Bertrand S, Brunet FG, Escriva H, et al. Evolutionary genomics of nuclear receptors: from twenty-five ancestral genes to derived endocrine systems. Mol Biol Evol 2004;21:1923-37.
25. Chen BD, Chen XC, Pan S, et al. TT genotype of rs2941484 in the human HNF4G gene is associated with hyperuricemia in Chinese Han men. Oncotarget 2017;8:26918-26.
26. Wang J, Zhang J, Xu L, et al. Expression of HNF4G and its potential functions in lung cancer. Oncotarget 2018;9:18018-28.
27. Sun H, Tian J, Xian W, et al. miR-34a inhibits proliferation and invasion of bladder cancer cells by targeting orphan nuclear receptor HNF4G. Dis Markers 2015;2015:879254.
28. Tian X, Ma J, Wang T, et al. Long Non-Coding RNA HOXA Transcript Antisense RNA Myeloid-Specific 1-HOXA1 Axis Downregulates the Immunosuppressive Activity of Myeloid-Derived Suppressor Cells in Lung Cancer. Front Immunol 2018;9:473.
29. Lin YH, Guo L, Yan F, et al. Long non-coding RNA HOTAIRM1 promotes proliferation and inhibits apoptosis of glioma cells by regulating the miR-873-5p/ZEB2 axis. Chin Med J (Engl) 2020;133:174-82.
30. Li DX, Fei XR, Dong YF, et al. The long non-coding RNA CRNDE acts as a ceRNA and promotes glioma malignancy by preventing miR-136-5p-mediated downregulation of Bcl-2 and Wnt2. Oncotarget 2017;8:88163-78.
31. Kiang KM, Zhang XQ, Zhang GP, et al. CRNDE Expression Positively Correlates with EGFR Activation and Modulates Glioma Cell Growth. Target Oncol 2017;12:353-63.
32. Liang Q, Li X, Guan G, et al. Long non-coding RNA, HOTAIRM1, promotes glioma malignancy by forming a ceRNA network. Aging (Albany NY) 2019;11:6805-38.

(English Language Editor: L. Huleatt)

Cite this article as: Wang WJ, Lu YJ, Li Y, Tang JQ, Wang H, Song W, Wang JJ, Huang YQ, Wang Y, Lian L. Construction of ceRNA networks with different types of *IDH1* mutation status in low-grade glioma patients. Ann Transl Med 2022;10(5):254. doi: 10.21037/atm-21-6983

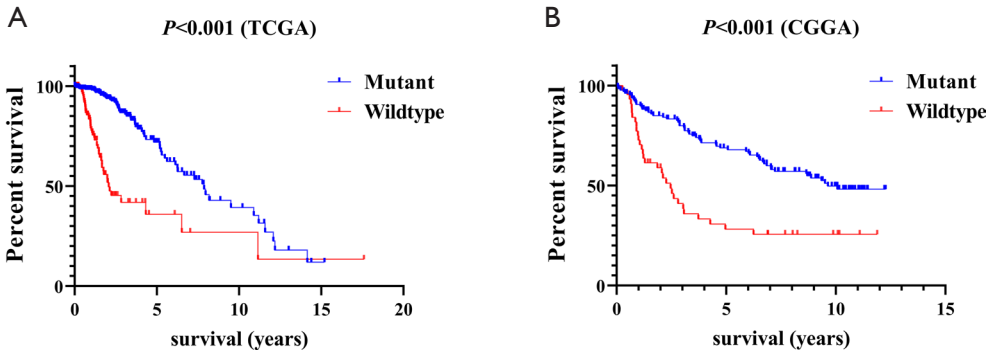

Figure S1 The survival analysis of different IDH1 mutation status groups. (A) TCGA; (B) CGGA. TCGA, The Cancer Genome Atlas; CGGA, Chinese Glioma Genome Atlas.

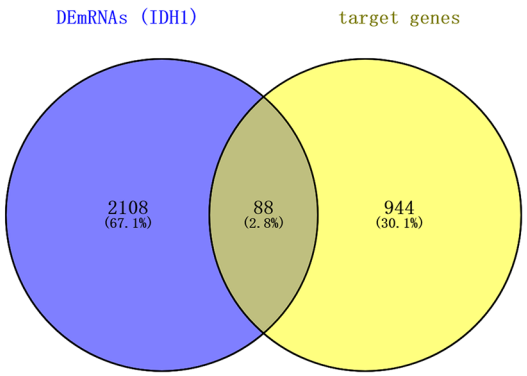

Figure S2 The Venn chart of DEmRNAs of the ceRNA network.

https://dx.doi.org/10.21037/atm-21-6983

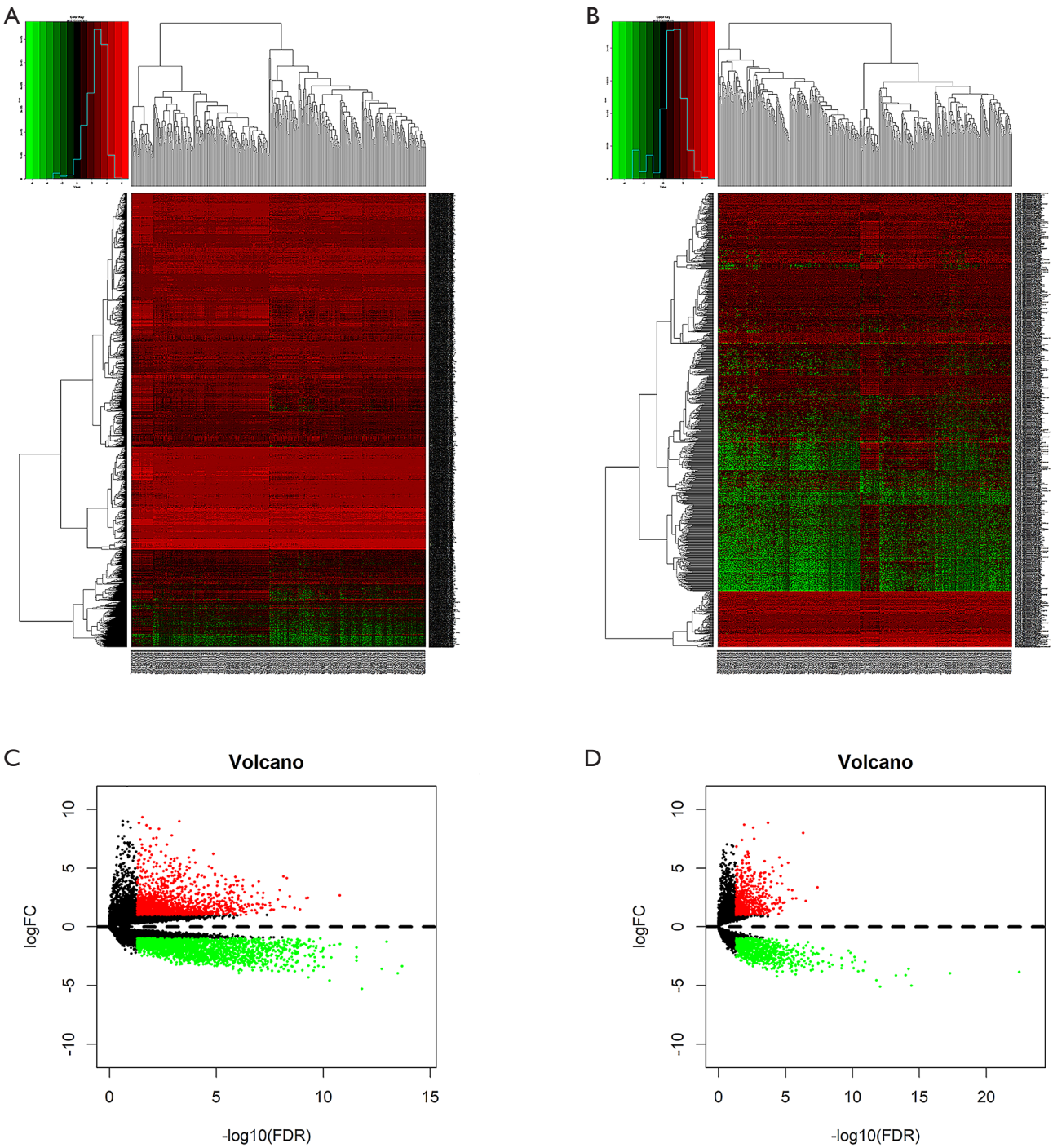

Figure S3 Identification of the DE^{LGG}lncRNAs and DE^{LGG}mRNAs in LGG and normal tissue samples: (A) Volcano plot of differentially expressed mRNAs, (B) lncRNAs. The red and green ones represent upregulated and downregulated RNAs, respectively. (C) Heatmap of DEmRNAs and (D) DElncRNAs. LGG, low-grade glioma.

https://dx.doi.org/10.21037/atm-21-6983

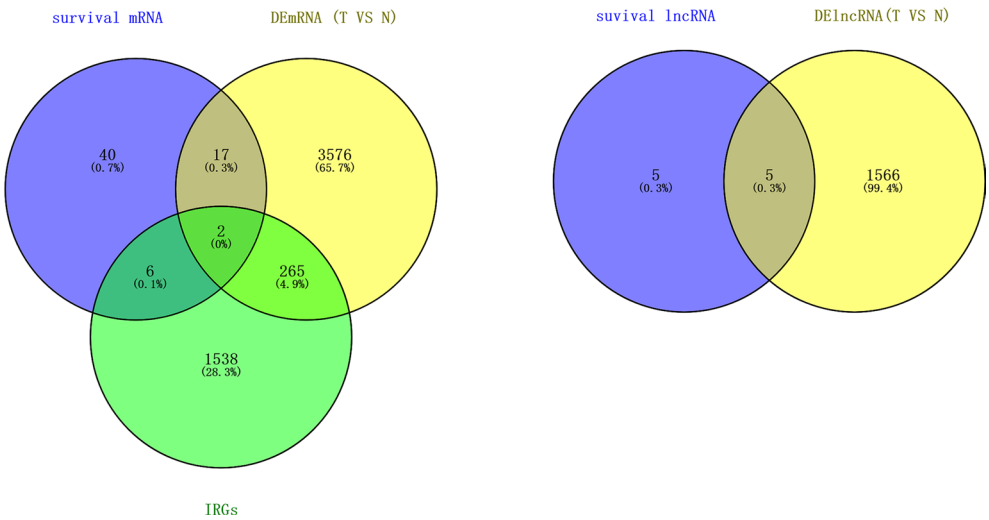

Figure S4 Venn diagram of DEmRNAs and DElncRNAs in new ceRNA network. (A) mRNA; (B) lncRNA.

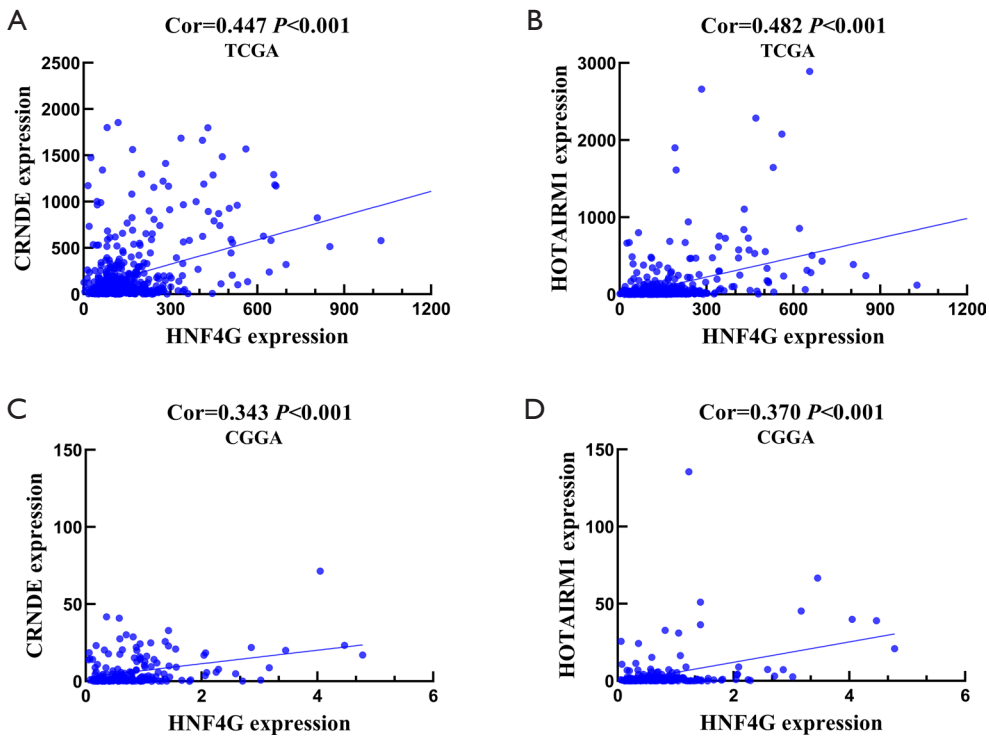

Figure S5 The relationship between the gene expression of *HNF4G* with *CRNDE* or *HOTAIRM1*. (A) The relationship between HNF4G with *CRNDE* in TCGA; (B) the relationship between *HNF4G* with HOTAIRM1 in TCGA; (C) the relationship between *HNF4G* with *CRNDE* in the CGGA; (D) the relationship between *HNF4G* with *HOTAIRM1* in the CGGA. TCGA, The Cancer Genome Atlas; CGGA, Chinese Glioma Genome Atlas.

https://dx.doi.org/10.21037/atm-21-6983

Table S1 Primer sequences for qRT-PCR

Primer	Sequence 5'-3'
HNF4G forward	TGCCATGCGGCTCTCTGATG
HNF4G reverse	CTTGACGGAGGCCGTTGGGTT
ANGPTL2 forward	TGTACCCCCAGGAGAGCCCG
ANGPTL2reverse	CGCCGGTACCACTGCTCCTC
CRNDE forward	CCTTTCCACCTC GTCGGTCT
CRNDE reverse	GCCTTAAAACT CCCAGTGTGC
HOTAIRM1 forward	CCAATGCGGATGATAGTG
HOTAIRM1 reverse	AACATCTGTGCGGGAACT
GLYCTK-AS1 forward	TCTACAGCCTTAACGAGGGCTAC
GLYCTK-AS1 reverse	AGCCTTCTCCATGACGTAGGCCA
GAPDH forward	CAACGAATTTGGCTACAGCA
GAPDH reverse	AGGGGTCTACATGGCAACTG

QT-PCR, quantitative real-time PCR.

Table S2 GO analysis

GO ID	Description	Genes	Count	P value
GO:0006351	transcription, DNA-templated	*HMX1, IRX5, E2F7, DMRT2, FASLG, RORB, VAX2, DEPDC1, HNF4G, SOX6, TOX3, VSX1, ARX, HOXA1, VDR, HOXC8, EBF2, SP6, NHLH2, ARNTL2, NR2F2, CHAF1B, DEDD2*	23	<0.001
GO:0003700	transcription factor activity, sequence-specific DNA binding	*IKZF3, E2F7, DMRT2, HOXD13, SOX4, RORB, VAX2, HNF4G, SOX6, VSX1, VDR, DLX2, HOXC8, ARNTL2, NR2F2*	15	<0.001
GO:0043565	sequence-specific DNA binding	*VDR, HOXA1, HOXC8, IKZF3, IRX5, DMRT2, RORB, SOX6, HNF4G, NR2F2, VSX1*	11	<0.001
GO:0000122	negative regulation of transcription from RNA polymerase II promoter	*ARX, VDR, DLX2, HOXC8, HMX1, E2F7, FASLG, VAX2, SOX6, HMGA2, NR2F2, EPO*	12	<0.001
GO:0045944	positive regulation of transcription from RNA polymerase II promoter	*IKZF3, E2F7, HOXD13, SOX4, DMRT2, SOX6, HGF, HMGA2, VDR, DLX2, HOXC11, EBF2, NHLH2, ARNTL2*	14	<0.001

DNA, deoxyribonucleic acid; GO, Gene Ontology; RNA, ribonucleic acid.

https://dx.doi.org/10.21037/atm-21-6983

Table S3 KEGG analysis

Pathway ID	Description	Gene	Count	P value
hsa04151	PI3K-Akt signaling pathway	*ANGPT1, HGF, FASLG, G6PC, EPO, LAMC1, EPHA2, ITGB3*	8	0.000168
hsa04360	Axon guidance	*EPHA7, EPHA5, EPHB2, SEMA3A, EPHA2*	5	0.001351
hsa04512	ECM-receptor interaction	*FREM2, LAMC1, ITGB3*	3	0.007601
hsa04974	Protein digestion and absorption	*COL5A3, COL21A1, KCNJ13*	3	0.009378
hsa04015	Rap1 signaling pathway	*ANGPT1, HGF, EPHA2, ITGB3*	4	0.015407
hsa04014	Ras signaling pathway	*ANGPT1, HGF, FASLG, EPHA2*	4	0.021417
hsa04060	Cytokine-cytokine receptor interaction	*FASLG, EPO, IL1RN, CXCL14*	4	0.045387
hsa04010	MAPK signaling pathway	*ANGPT1, HGF, FASLG, EPHA2*	4	0.045862
hsa05206	MicroRNAs in cancer	*SOX4, HMGA2, SPRY2, ITGB3*	4	0.048322
hsa04510	Focal adhesion	*HGF, LAMC1, TGB3*	3	0.048544

ECM, extracellular matrix; KEGG, Kyoto Encyclopedia of Genes and Genomes; MAPK, mitogen-activated protein kinase; PI3K. phosphatidylinositol 3'-kinase.

https://dx.doi.org/10.21037/atm-21-6983